Decadal variability of twentieth-century El Niño and La Niña occurrence from observations and IPCC AR4 coupled models

Xin Wang,[1] Dongxiao Wang,[1] and Wen Zhou[2]

Received 27 February 2009; revised 19 April 2009; accepted 22 April 2009; published 2 June 2009.

[1] This study investigates the decadal variability of El Niño and La Niña occurrence in observations and examines that variability in a set of 20th Century climate simulations (20C3M) of coupled general circulation models (CGCMs) in the Intergovernmental Panel on Climate Change (IPCC) Fourth Assessment Report (AR4).Wavelet analysis reveals that the observed frequency of El Niño events displays significant decadal variability with a period of about 12 years during 1920–1940, whereas the frequency of La Niña events shows significant decadal variations with a spectral peak at 16 years throughout the 20th century. Moreover, the frequencies of El Niño and La Niña events are influenced by different factors that are responsible for planetary teleconnections. The frequency of El Niño events is related the Atlantic Multidecadal Oscillation (AMO), while that of the La Niña events is associated with the Pacific Decadal Oscillation (PDO). Among the 15 IPCC AR4 CGCMs surveyed, csiro and miroc_medres CGCMs can reproduce the decadal variability of ENSO activity, and simulate partly its relationship with the Pacific and north Atlantic SSTa. These results will help us to further understand the important roles of the North Atlantic and North Pacific in ENSO variations. **Citation:** Wang, X., D. Wang, and W. Zhou (2009), Decadal variability of twentieth-century El Niño and La Niña occurrence from observations and IPCC AR4 coupled models, *Geophys. Res. Lett.*, *36*, L11701, doi:10.1029/2009GL037929.

1. Introduction

[2] The characteristics of El Niño-Southern Oscillation (ENSO) display significant decadal variability, in terms of amplitude, oscillation period, onset time and propagation of sea-surface temperature anomalies (SSTa) along the equator [e.g., *Wang*, 1995; *An and Wang*, 2000; *Zhang et al.*, 2008]. In addition, the occurrence of ENSO events exhibits low-frequency variability. *Trenberth and Hoar* [1996] first pointed out the tendency for more frequent El Niño events and fewer La Niña events since the late 1970s. Using monthly resolved coral δ^{18}O records, *Cobb et al.* [2003] concluded some 17th-century El Niño events rival the 1997 El Niño event in severity. They also noted that ENSO events in the 17th century were more frequent than those in the late 20th century.

[3] The low-frequency variability of ENSO is associated with the Indian, Pacific and Atlantic SST variations [e.g., *Behera and Yamagata*, 2003; *Verdon and Franks*, 2006; *Luo et al.*, 2005; *Dong et al.*, 2006]. Using the data inferred from paleoclimate records over the past 400 years, *Verdon and Franks* [2006] suggested that phase change in the Pacific Decadal Oscillation (PDO) has a positive propensity to coincide with changes in the frequency of ENSO events. Coupled modeling studies have shown that the North Atlantic SSTa may also influence ENSO variability via atmospheric bridge [*Dong et al.*, 2006] or via oceanic wave adjustment [*Timmermann et al.*, 2005]. The analyses of observational data suggested that the pronounced subsurface ocean temperature anomalies can influence the decadal ENSO-like variation [*Luo and Yamagata*, 2001]. Simulations from ocean model also indicated that the decadal variability of temperature along the equator originates from subsurface spiciness anomalies in the South Pacific [*Luo et al.*, 2005]. In this paper, we will continue to investigate the low-frequency variability of ENSO occurrence and its linkage to the PDO and AMO.

[4] The ENSO simulations of coupled general circulation models (CGCMs) in the Intergovernmental Panel on Climate Change (IPCC) Fourth Assessment Report (AR4) have been evaluated by many studies [e.g., *van Oldenborgh et al.*, 2005; *Capotondi et al.*, 2006; *Lin*, 2007]. For example, *van Oldenborgh et al.* [2005] considered the overall ENSO properties in the models for the IPCC AR4: amplitude, pattern, and spectrum. *Capotondi et al.* [2006] focused on the spatial structure and spectral characteristics of ENSO in these models. However, the ability of CGCMs to simulate the frequency of ENSO event occurrence is not known. Knowing such model ability is important because if some of these CGCMs can simulate the frequency of ENSO events well, it may help us to reveal the physical mechanism influencing the frequency of ENSO event occurrence.

[5] The purpose of this study is to analyze the frequency of ENSO event occurrence and associated planetary teleconnections in observational datasets and in simulations by 15 CGCMs in the IPCC AR4. The validation datasets, models and diagnostic methods are presented in section 2. Results are described in section 3, followed by summary and discussion in section 4.

2. Datasets and Method

[6] In order to describe variations of the frequency of El Niño and La Niña event occurrence, the indices of El Niño and La Niña activities are defined as the number of El Niño and La Niña events in a running 7-yr window [*Cobb et al.*, 2003]. The observed ENSO events are those selected by the Japan Meteorological Agency (JMA; http://coaps.fsu.edu/jma.shtml), using 5-month running mean of spatially-

[1]Key Laboratory of Tropical Marine Environmental Dynamics, South China Sea Institute of Oceanology, Chinese Academy of Sciences, Guangzhou, China.
[2]Guy Carpenter Asia-Pacific Climate Impact Centre, City University of Hong Kong, Hong Kong, China.

0094-8276/09/2009GL037929$05.00

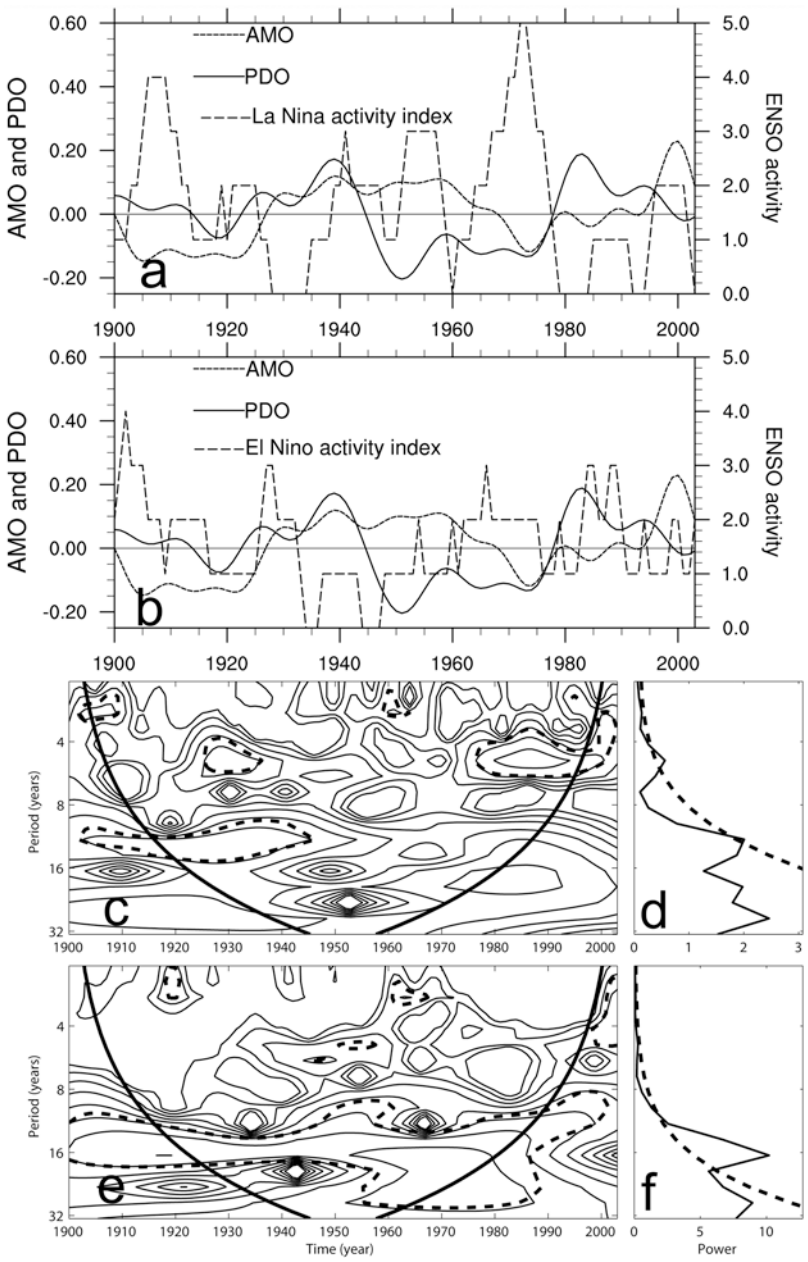

Figure 1. (a) The index of La Niña activity and the normalized 10yr low-pass filtered AMO (dotted) and PDO (solid). The dashed lines indicate the mean of the La Niña activity. (b) The index of El Niño activity and the normalized 10yr low-pass filtered AMO (dotted) and PDO (solid). The dashed lines indicate the mean of the El Niño activity. (c and e) Wavelet power spectra of the indices of El Niño and La Niña activities using the Morlet wavelet. The thick dashed contour encloses regions of greater than 95% confidence for a red-noise process. (d and f) Global wavelet spectra of the indices El Niño and La Niña activity. The dashed lines indicate 95% confidence level.

averaged SSTa over the tropical Pacific region of 4°S–4°N and 150°–90°W. If the index values are 0.5°C or greater (−0.5°C or lower) for 6 consecutive months (including October, November and December), the period of October through the following September is categorized as El Niño (La Niña) event. These ENSO activity indices are used to validate the model simulations in this study.

[7] The monthly UK Met Office/Hadley Centre's Sea Ice and SST (HadISST) [*Rayner et al.*, 2003] with horizontal resolution of 1° by 1° are used. The monthly PDO index is the leading principal component of monthly SSTa in the Pacific Ocean north of 20°N [*Mantua et al.*, 1997]. The Atlantic Multidecadal Oscillation (AMO) [*Kerr*, 2000] index is defined by the averaged SSTa over the region 0°–60°N, 75°W–7.5°W. Due to ENSO activity index is defined with running 7-yr window, the PDO and AMO indices are both 10-yr low-pass filtered in this study. Although more than 20 CGCMs participated in the IPCC AR4 project, only 15 of the Climate of the 20th Century (20C3M) simulations are analyzed in this study because the remaining CGCMs have much fewer ENSO events than observed (e.g., El Niño occurred only once in giss_e_r

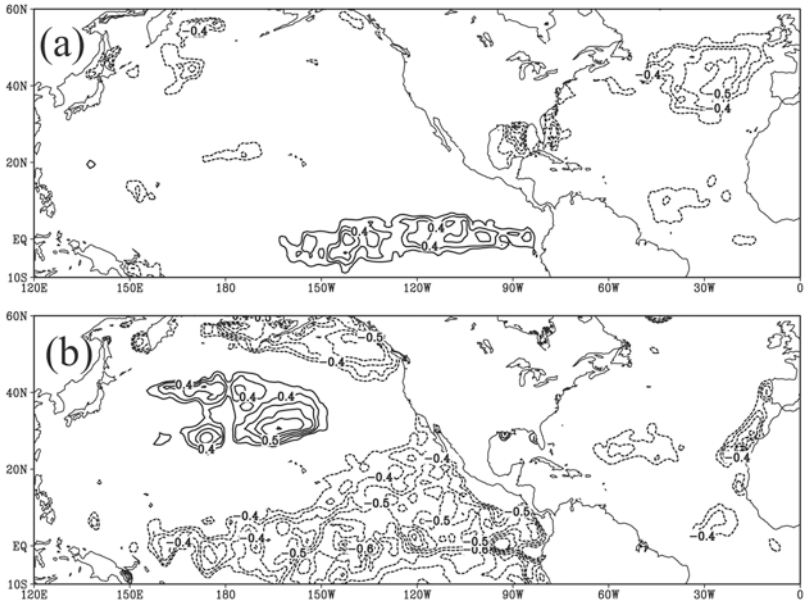

Figure 2. The correlation coefficient patterns between (a) El Niño, (b) La Niña activity and contemporaneous 7-yr running-averaged SSTa. Only values above the 95% confidence level are used. Note that the degree of freedom is 30 due to 7-yr moving average.

and giss_aom). All datasets cover the 104 years from 1900 to 2003.

[8] The variability of El Niño and La Niña activity indices is examined using the wavelet analysis program developed by *Torrence and Compo* [1998]. The Morlet wavelet is used as the mother wavelet.

3. Results

[9] Firstly, the ENSO activity indices from observational dataset are exhibited in Figure 1. The index of La Niña activity shows that during 1905–1925 and 1940–1978 the number of La Niña events was generally above the normal level, whereas it was slightly below the normal level in 1926–1940 and after 1980 (Figure 1a). It is well known that the PDO was at its negative phase during 1910–1920 and 1945–1977, and at its positive phase in 1921–1945 and after 1980 [*Minobe*, 1997]. The correlation coefficient between the La Niña activity index and the PDO index is −0.5 at the 95% confidence level. Therefore, the variations of La Niña activity coincide with those of the PDO phase, agreeing well with previous studies [*Verdon and Franks*, 2006]. Moreover, the correlation coefficient between the La Niña activity index and the AMO is only −0.24, suggesting that La Niña activity is much less associated with the North Atlantic SSTa. However, it is worth noting that the El Niño activity index does not have a propensity to coincide with changes of the PDO phases. During both negative phases (1960–1975) and positive phases (1980–1990) of the PDO, the number of El Niño events was more than the normal level. During 1965–1975 when the PDO was in its negative phases, El Niño events occurred as frequently as when the PDO was in its positive phases during 1980–1990. The number of El Niño events was less than the normal level not only when the PDO was in its negative phases during 1945–1960 but also when the PDO was in its positive phases during 1930–1945. Moreover, the correlation coefficient between the El Niño activity index and the PDO index is only 0.04, indicating that El Niño activity does not correlate with the PDO. Actually, the variations of the index of El Niño activity in Figure 1b seem to coincide well with the phase changes of the AMO, whose warm phases occurred during 1925–1960 and cold phases during 1900–1925 and 1965–1990 (Figure 1b). The El Niño activity index is correlated significantly with the AMO index, with a correlation coefficient of −0.35. Based on results from a CGCM, *Dong et al.* [2006] suggested that the warm AMO lead to weaker ENSO variability via atmospheric bridge that conveys the influence of the Atlantic Ocean to the tropical Pacific.

[10] The wavelet analysis is applied to identify the difference of the variations between El Niño and La Niña activities. It is found that El Niño activity has significant decadal oscillation occurred in 1920–1940 (Figure 1c). The global wavelet spectra of El Niño activity index show also decadal oscillation with a period of about 12 years (Figure 1d). Different from the variations of El Niño activity, Figure 1e indicates that the decadal variations of La Niña activity were always significant during the 20th century, and the dominant period of La Niña activity variations became longer after 1960. The results of the global wavelet spectra show that La Niña activity exhibits significant decadal variations with a spectral peak at 16 years (Figure 1f), longer than that of El Niño activity.

[11] To further examine the relationship between the El Niño/La Niña activity and the AMO/PDO, correlation coefficient patterns between the ENSO activity and contemporaneous 7-yr running-averaged SSTa are shown in Figure 2. In Figure 2a, the correlations between the El Niño activity index and SSTa are large in two regions, the eastern tropical Pacific and the North Atlantic (50°W–10°W, 30°N–50°N). In contrast, significant correlations for the

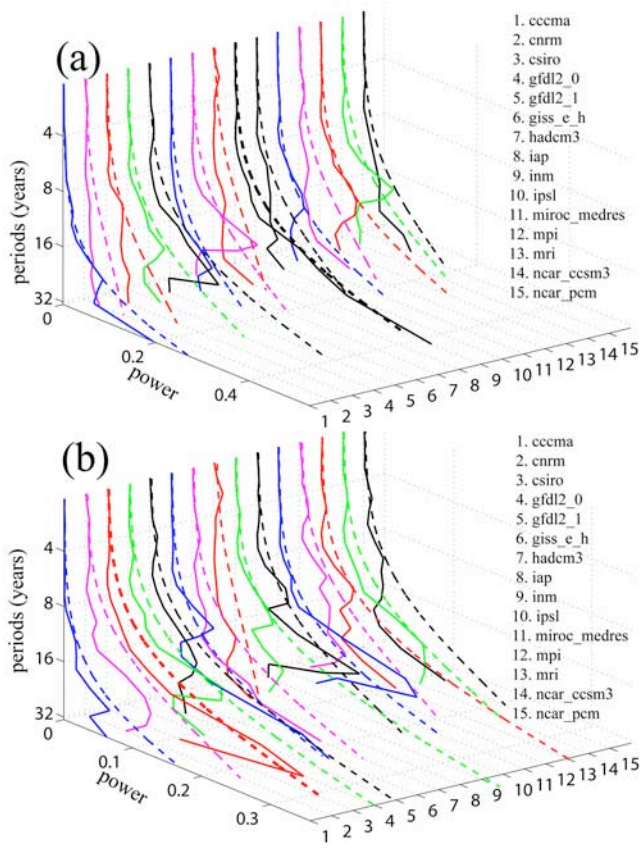

Figure 3. The global wavelet spectra of the indices (a) El Niño and (b) La Niña activity for the 15 IPCC AR4 CGCMs. The dashed lines indicate 95% confidence level. The mother wavelet is the Morlet wavelet.

La Niña activity index and SSTa are located in the North Pacific (160°E–150°W, 25°N–40°N) and eastern tropical Pacific, similar to the positive PDO phase pattern (Figure 2b). Therefore, the planetary teleconnections related to El Niño and La Niña activities differ from each other.

[12] We next examine the decadal variability of ENSO activity in the 15 IPCC AR4 CGCMs. According to the global wavelet spectral analysis, the indices of El Niño activity from csiro, hadcm3, miroc_medres and ncar_ccsm3 show significant decadal variations, while the other CGCMs do not have any statistically-significant periods (Figure 3a). Note that except for csiro the dominant periods in hadcm3, miroc_medres and ncar_ccsm3 are longer than the observed. Moreover, the results of wavelet spectra show that significant decadal oscillations in csiro and miroc_medres occurred before 1920, and those in hadcm3 and ncar_ccsm3 were during 1920–1940 (not shown). The latter is similar to observations. The indices of La Niña activity from five of the CGCMs, including csiro, gfdl2.0, ipsl, miroc_medres and ncar_ccsm3, display significant decadal oscillations with spectral peaks between 16–20 years (Figure 3b), similar to observations; the other models fail to reproduce these observed periods. It is noted that the significant periods in csiro, ipsl, miroc_medres and ncar_ccsm3 are longer than those observed. Using wavelet spectra, the decadal oscillations in csiro, gfdl2.0, and ispl are significant in 1910–1970 as observed, whereas the oscillations are significant in 1920–1950 for miroc_medres and in 1950–1970 for ncar_ccsm3 (not shown). Thus, although none of these CGCMs can produce similar variations of El Niño and La Niña activities as observed, three of the CGCMs, including csiro, miroc_medres and ncar_ccsm3, can produce the dominant periods of both El Niño and La Niña activities.

[13] It would be interesting to see how many of the six CGCMs (csiro, gfdl2.0, hadcm3, ipsl, miroc_medres and ncar_ccsm3 CGCMs) that can simulate the dominant periods of El Niño or La Niña activities can also reproduce the linkage between the El Niño activity and the AMO or the linkage between the La Niña activity and the PDO as shown in observations. Figure 4 shows the correlation coefficient patterns between El Niño/La Niña activities and SSTa in these CGCMs. It is clear that the indices of El Niño activity correlate significantly positively with the eastern tropical Pacific SSTa in these models. It is noted that correlations between the El Niño activity index and SSTa in csiro and miroc_medres (Figures 4a and 4i) are significantly-negative in the central North Pacific and significantly-positive in the tropical Pacific, which is similar to the positive PDO phase. Moreover, the indices of El Niño activity for all six CGCMs that can simulate the dominant periods of El Niño or La Niña activities are also correlated significantly with the Atlantic SSTa. Different from the observations (Figure 2a), there are significantly-positive correlations between the indices of El Niño activity and the Atlantic SSTa south of 40°N for gfdl2.0, hadcm3, ipsl, miroc_medres and ncar_ccsm3 (Figures 4c, 4e, 4g, 4i, and 4k). For csiro and miroc_medres (Figure 4a and 4i), the indices of El Niño activity correlate significantly negatively with the North Atlantic SSTa (north of 40°N), coinciding with the observations. The region with significantly-negative correlation coefficients for miroc_medres (Figure 4i) is much larger than those for csiro (Figure 4a). Thus, there is no one CGCMs which can simulate completely the relationship between El Niño activity and the Pacific and Atlantic SSTa. Csiro and miroc_medres can reproduce partly the relationship between El Niño activity and the Pacific and Atlantic SSTa.

[14] Evidently, the indices of La Niña activity correlate significantly negatively with the eastern tropical Pacific SSTa for all six CGCMs that can simulate the dominant periods of El Niño or La Niña activities (Figure 4). It is noted that except csiro model, the patterns of significant correlation coefficients between the indices of La Niña activity and the Pacific SSTa for the five CGCMs do not display the PDO pattern as well as the observed (Figure 2b). However, for csiro, the area positive correlated with the index of La Niña activity in the North Pacific is less than the observed (Figure 4b). For ipsl and miroc_medres (Figures 4h and 4j), the significant correlation coefficient patterns with the indices of La Niña activity and the Atlantic SSTa are similar to the observations (Figure 2b). Only SSTa south of 20°N or in the east coast of the Atlantic are correlated significantly negatively with the indices of La Niña activity in ipsl and miroc_medres (Figures 4h and 4j). Therefore, these CGCMs are failure to simulate the relationships between La Niña activity and the Pacific and Atlantic SSTa. Only csiro and miroc_medres

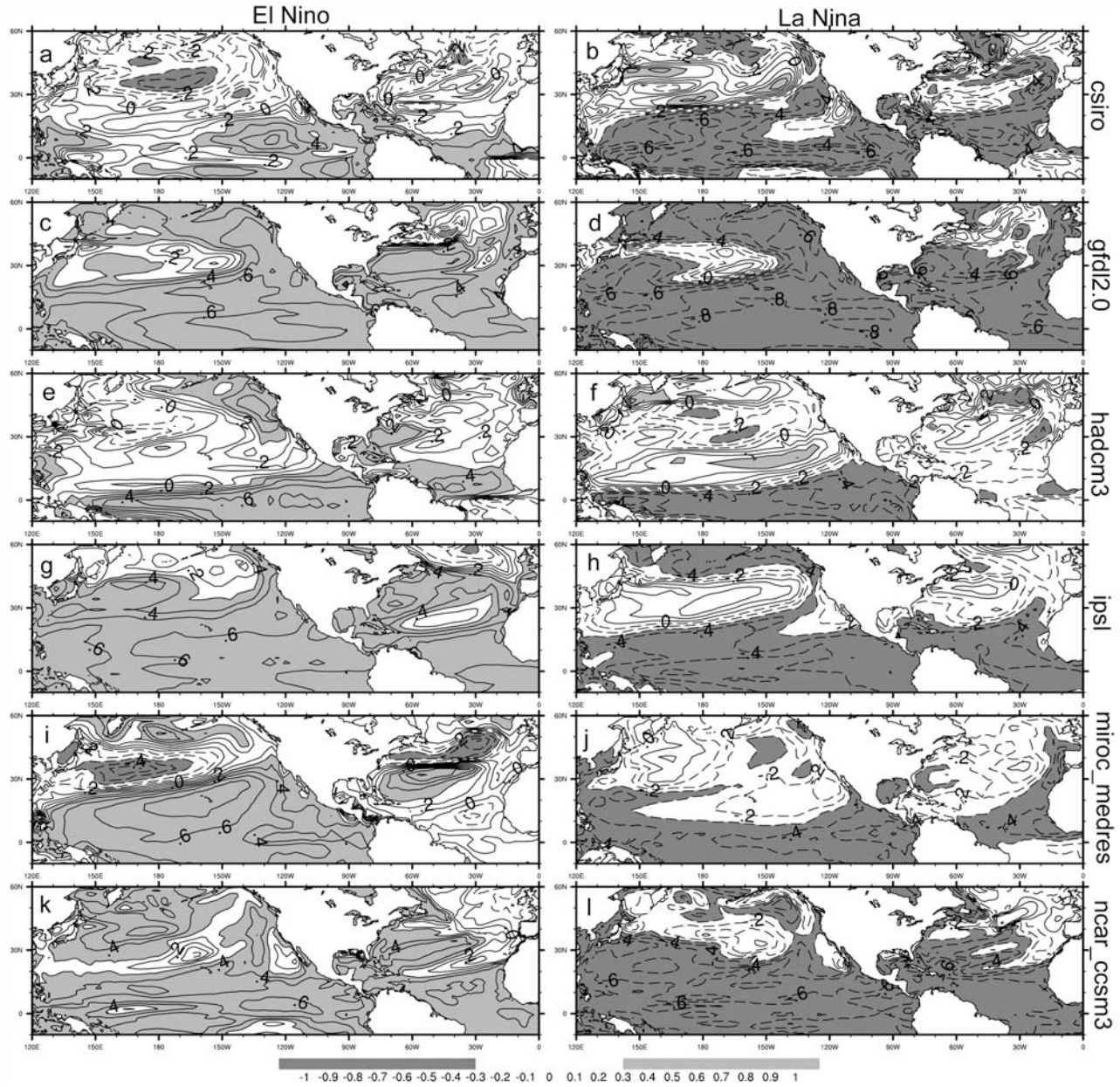

Figure 4. The correlation coefficient patterns between the indices of (left) El Niño/(right) La Niña activity and contemporaneous 7-yr running average SSTa for csiro, gfdl2.0, hadcm3, ipsl, miroc_medres and ncar_ccsm3. The shading are above the 95% confidence level.

can simulate partly the relationship between La Niña activity and the Pacific and Atlantic SSTa to some degree.

4. Summary

[15] This study shows the change of ENSO activity based on observed datasets, and evaluates the simulations by 15 IPCC AR4 CGCMs. Using wavelet analyses of observations, the indices of both El Niño and La Niña activities display significant decadal variability. The index of La Niña activity displays a spectral peak at 16 years in the 20th century, much longer than the peak for the index of El Niño (about 12 years). The observational datasets also show that the changes in El Niño and La Niña activities are related with different planetary teleconnections. El Niño activity is associated significantly with the eastern tropical Pacific and North Atlantic SSTa, whereas La Niña activity is closely related to changes in PDO phases.

[16] The performances of the 15 IPCC AR4 CGCMs differ greatly in terms of their simulated ENSO activity. There are only six CGCMs that can produce the significant decadal variations of El Niño or La Niña activity, including csiro, gfdl2.0, hadcm3, ipsl, miroc_medres and ncar_ccsm3. Among them, csiro, miroc_medres and ncar_ccsm3 can produce the dominant periods of both El Niño and La Niña activities. Unfortunately, the results from these CGCMs could not reproduce completely the relationship between the ENSO activities and the Pacific and Atlantic SSTa. Only csiro and miroc_medres can reproduce partly the relationship between El Niño (La Niña) activity and the eastern

tropical Pacific and North Atlantic SSTa (PDO). Therefore, although these CGCMs cannot simulate exactly ENSO activity as observed, we are encouraged that csiro and miroc_medres can simulate the variations of ENSO activity, which will help us to further understand the physical mechanisms of how the Pacific and Atlantic SSTs impact ENSO variability and may improve the ability of ENSO forecast.

[17] **Acknowledgments.** This research is sponsored by the Chinese Academy of Sciences (grant KZSW2-YW-214), the MOST of China (grant 2006CB403604), and the Natural Science Foundation of China (grants U0733002 and 40625017) and partly supported by City University of Hong Kong (grant 7002136). We thank two anonymous reviewers for valuable comments.

References

An, S.-I., and B. Wang (2000), Interdecadal change of the structure of the ENSO mode and its impact on the ENSO frequency, *J. Clim.*, *13*, 2044–2055.

Behera, S. K., and T. Yamagata (2003), Influence of the Indian Ocean Dipole on the Southern Oscillation, *J. Meteorol. Soc. Jpn.*, *81*, 169–177.

Capotondi, A., A. Wittenberg, and S. Masina (2006), Spatial and temporal structure of tropical Pacific interannual variability in 20th century coupled simulations, *Ocean Modell.*, *15*, 274–298.

Cobb, K. M., C. D. Charles, H. Cheng, and R. L. Edwards (2003), El Niño/Southern Oscillation and tropical Pacific climate during the last millennium, *Nature*, *424*, 271–276.

Dong, B., R. T. Sutton, and A. A. Scaife (2006), Multidecadal modulation of El Niño–Southern Oscillation (ENSO) variance by Atlantic Ocean sea surface temperatures, *Geophys. Res. Lett.*, *33*, L08705, doi:10.1029/2006GL025766.

Kerr, R. A. (2000), A North Atlantic climate pacemaker for the centuries, *Science*, *288*, 1984–1986.

Lin, J. L. (2007), Interdecadal variability of ENSO in 21 IPCC AR4 coupled GCMs, *Geophys. Res. Lett.*, *34*, L12702, doi:10.1029/2006GL028937.

Luo, J.-J., and T. Yamagata (2001), Long-term El Niño-Southern Oscillation (ENSO)-like variation with special emphasis on the South Pacific, *J. Geophys. Res.*, *106*, 22,211–22,227.

Luo, Y., L. M. Rothstein, R.-H. Zhang, and A. J. Busalacchi (2005), On the connection between South Pacific subtropical spiciness anomalies and decadal equatorial variability in an ocean general circulation model, *J. Geophys. Res.*, *110*, C10002, doi:10.1029/2004JC002655.

Mantua, N. J., S. R. Hare, Y. Zhang, J. M. Wallace, and R. C. Francis (1997), A Pacific interdecadal climate oscillation with impacts on salmon production, *Bull. Am. Meteorol. Soc.*, *78*, 1069–1079.

Minobe, S. (1997), A 50–70 year climatic oscillation over the North Pacific and North America, *Geophys. Res. Lett.*, *24*, 683–686.

Rayner, N. A., D. E. Parker, E. B. Horton, C. K. Folland, L. V. Alexander, D. P. Rowell, E. C. Kent, and A. Kaplan (2003), Global analyses of sea surface temperature, sea ice, and night marine air temperature since the late nineteenth century, *J. Geophys. Res.*, *108*(D4), 4407, doi:10.1029/2002JD002670.

Timmermann, A., S.-I. An, U. Krebs, and H. Goosse (2005), ENSO suppression due to weakening of the North Atlantic thermohaline circulation, *J. Clim.*, *18*, 3122–3138.

Torrence, C., and G. P. Compo (1998), A practical guide to wavelet analysis, *Bull. Am. Meteorol. Soc.*, *79*, 61–78.

Trenberth, K. E., and T. J. Hoar (1996), The 1990–1995 El Niño-Southern Oscillation event: Longest on record, *Geophys. Res. Lett.*, *23*, 57–60.

van Oldenborgh, G. J., S. Y. Philip, and M. Collins (2005), El Niño in a changing climate: A multi-model study, *Ocean Sci.*, *1*, 81–95.

Verdon, D. C., and S. W. Franks (2006), Long-term behaviour of ENSO: Interactions with the PDO over the past 400 years inferred from paleoclimate records, *Geophys. Res. Lett.*, *33*, L06712, doi:10.1029/2005GL025052.

Wang, B. (1995), Interdecadal changes in El Niño onset in the last four decades, *J. Clim.*, *8*, 267–285.

Zhang, R.-H., J. Busalacchi, and D. G. DeWitt (2008), The roles of atmospheric stochastic forcing (SF) and oceanic entrainment temperature (T_e) in decadal modulation of ENSO, *J. Clim.*, *21*, 674–704.

D. Wang and X. Wang, Key Laboratory of Tropical Marine Environmental Dynamics, South China Sea Institute of Oceanology, Chinese Academy of Sciences, 164 West Xingang Road, Guangzhou 510301, China. (dxwang@scsio.ac.cn)

W. Zhou, Guy Carpenter Asia-Pacific Climate Impact Centre, City University of Hong Kong, Chee Avenue, Kowloon, Hong Kong, China.